AD-A197 447

AN EFFICIENT METHOD FOR PREDICTING THE VIBRATORY RESPONSE OF LINEAR STRUCTURES WITH FRICTION INTERFACES
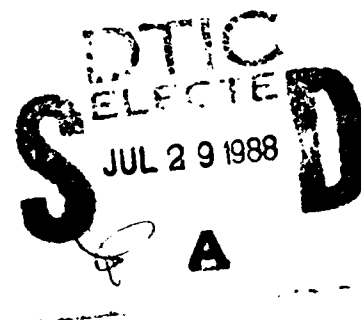
VOLUME I - Theory and Application

Enrique Bazan-Zurita, Jacobo Bielak, and Jerry H. Griffin
Carnegie Institute of Technology
Carnegie Mellon University
Pittsburgh, Pennsylvania 15213
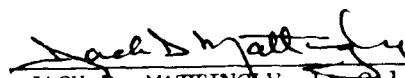
29 March 1988

DTIC
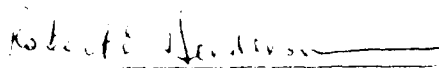SELECTED
JUL 2 9 1988
S D
A

NOTICE

When Government drawings, specifications, or other data are used for any purpose other than in connection with a definitely Government-related procurement, the United States Government incurs no responsibility or any obligation whatsoever. The fact that the government may have formulated or in any way supplied the said drawings, specifications, or other data, is not to be regarded by implication, or otherwise in any manner construed, as licensing the holder, or any other person or corporation; or as conveying any rights or permission to manufacture, use, or sell any patented invention that may in any way be related thereto.

This report is releasable to the National Technical Information Service (NTIS). At NTIS, it will be available to the general public, including foreign nations.

This technical report has been reviewed and is approved for publication.

WILLIAM A. STANGE
Project Engineer
Components Branch
Turbine Engine Division

FOR THE COMMANDER

JACK D. MATTINGLY, Lt Col, USAF
Chief, Components Branch
Turbine Engine Division

ROBERT E. HENDERSON
Deputy for Technology
Turbine Engine Division
Aero Propulsion Laboratory

If your address has changed, if you wish to be removed from our mailing list, or if the addressee is no longer employed by your organization please notify AFWAL/POTA, WPAFB, OH 45433-6563 to help us maintain a current mailing list.

Copies of this report should not be returned unless return is required by security considerations, contractual obligations, or notice on a specific document.

REPORT DOCUMENTATION PAGE

1. REPORT SECURITY CLASSIFICATION		1b. RESTRICTIVE MARKINGS		
UNCLASSIFIED				
2a. SECURITY CLASSIFICATION AUTHORITY		3. DISTRIBUTION/AVAILABILITY OF REPORT		
		Approval for Public Release, distribution unlimited.		
2b. DECLASSIFICATION/DOWNGRADING SCHEDULE				
4. PERFORMING ORGANIZATION REPORT NUMBER(S)		5. MONITORING ORGANIZATION REPORT NUMBER(S)		
R-86-158, R-86-159, R-86-160		AFWAL-TR-86-2119, Volume I		
6a. NAME OF PERFORMING ORGANIZATION	6b. OFFICE SYMBOL (If applicable)	7a. NAME OF MONITORING ORGANIZATION		
Carnegie Mellon University		Aero Propulsion Laboratory (AFWAL/POTA) Air Force Wright Aeronautical Laboratories		
6c. ADDRESS (City, State and ZIP Code)		7b. ADDRESS (City, State and ZIP Code)		
Carnegie Mellon University Pittsburgh, PA 15213		AFWAL/POTA Wright-Patterson AFB OH 45433-6563		
8a. NAME OF FUNDING/SPONSORING ORGANIZATION	8b. OFFICE SYMBOL (If applicable)	9. PROCUREMENT INSTRUMENT IDENTIFICATION NUMBER		
		F33615-83-K-2316		

8c. ADDRESS (City, State and ZIP Code)	10. SOURCE OF FUNDING NOS			
	PROGRAM ELEMENT NO	PROJECT NO	TASK NO	WORK UNIT NO
11. TITLE (Include Security Classification) An efficient method for predicting the (OVER)	61102F	2307	S2	12

12. PERSONAL AUTHOR(S)
Bazan-Zurita, E., Bielak, J., and Griffin, J.H.

13a. TYPE OF REPORT	13b. TIME COVERED	14. DATE OF REPORT (Yr, Mo., Day)	15. PAGE COUNT
FINAL	FROM May 83 TO Oct 86	88 MARCH 29	44

16. SUPPLEMENTARY NOTATION

17.	COSATI CODES		18. SUBJECT TERMS (Continue on reverse if necessary and identify by block number)
FIELD	GROUP	SUB GR	

19. ABSTRACT (Continue on reverse if necessary and identify by block number)

A simple methodology to study the steady-state response of systems consisting of linear elastic substructures connected by friction interfaces is presented. Assuming that only the first Fourier components of the friction forces contribute significantly to the system response, the differential equations of motion are transformed into a system of algebraic complex equations. An efficient linearized procedure is then developed for solving these equations for different normal loads in the friction interfaces. As part of the solution procedure, a criterion to determine the slip-to-stuck transitions in the joint is proposed. Within the assumption that the response is harmonic, any desired accuracy can be obtained with this methodology. Data structures and algorithms for the automatic formulation of the system of algebraic complex equations are also developed. Selected numerical examples are presented to illustrate practical applications and the relevant features of the methodology. Due to its simplicity, this methodology is
(OVER)

20. DISTRIBUTION/AVAILABILITY OF ABSTRACT	21. ABSTRACT SECURITY CLASSIFICATION
UNCLASSIFIED/UNLIMITED ☒ SAME AS RPT ☐ DTIC USERS ☐	UNCLASSIFIED
22a. NAME OF RESPONSIBLE INDIVIDUAL	22b. TELEPHONE NUMBER (Include Area Code)	22c. OFFICE SYMBOL
WILLIAM A. STANGE	(513) 255-2081	AFWAL/POTA

DD FORM 1473, 83 APR   EDITION OF 1 JAN 73 IS OBSOLETE   UNCLASSIFIED

ii   The vibratory response of linear structures with friction interfaces, Volume i
Theory and Application.

iii. particularly appropriate for performing parametric studies that require solutions
for many values of normal loads.

ACKNOWLEDGEMENTS

iii

Table of Contents

List of Figures

1 Introduction

One important consideration in the design of gas turbine engines is limiting the amplitudes of steady-state vibrations of its components in order to prevent failures due to high cycle fatigue. The most widely used damping devices incorporate especially designed friction interfaces which dissipate energy and reduce high frequency vibrations to an acceptable level. The study of steady-state vibrations of structures with so-called frictional dampers has attracted the attention of many investigators. The first analytical solution for a single-degree-of-freedom system with a Coulomb frictional joint was presented by Den Hartog [5]. The most relevant contributions until 1979 are discussed by Plunkett [11]. More recently, further analytical and experimental research has been reported by Griffin and coworkers [7, 13, 4], Muszynska et al [10], Srinivasan et al [17], Dominic et al [6], and Soni and Bogner [14], among others.

Most analytical studies are limited to cases with one friction joint only, mainly due to the difficulties of solving the nonlinear differential equations which result from the mathematical models. The available mathematical models and methods of solution cannot be easily extended to problems with several friction joints, and their results do not explain completely all the experimentally observed phenomena. For these reasons, a more efficient and rational utilization of friction dampers still requires additional experimental and analytical research.

In this report we present a simple, approximate, yet accurate, methodology for studying the steady-state response of structures containing friction interfaces, but which are otherwise linear. The procedures that are developed result in systems of nonlinear equations that would be prohibitively expensive to solve if the global problem were formulated directly. This difficulty was avoided by exploiting the linearity of the individual subsystems utilizing finite element substructuring techniques. The substructuring approach has been widely used in mechanics to solve static problems [12], as well as dynamic problems [8, 9]. In fact, this approach was used to analyze shrouded blades in [16]. The work described in this report is significantly different in that we incorporate friction constraints at the interfaces. In linear analyses it is possible to back calculate a coefficient of viscous or structural damping to produce the same peak response as that obtained with friction damping. This value, however, will depend on the level of excitation and on the normal force at the interface; it cannot be obtained directly from the physics of the problem and can only be calculated once the response is known. For example, in a structure that contains a friction interface no damping occurs if the excitation is small since the joint does not slip. However, for larger levels of excitation, the static friction in the joint can be overcome and rubbing can dissipate a significant amount of energy. Clearly, both conditions cannot be represented by a single value of equivalent viscous or structural damping. In the approach presented here, the nonlinear damping dissipated by friction is calculated directly for any level of excitation without resorting to "calibrating" the model

The organization of the report is as follows. First, the differential equations governing the motion of the system under study are formulated in terms of the complete set of system displacements. A methodology to obtain approximate solutions of these equations is presented next, based on the assumption that only the first Fourier component of the tangential forces in the friction joints has a significant participation in the system response. The problem is ultimately reduced to the solution of an algebraic system of equations relating the complex variable representation of the relative displacements and the tangential forces in the friction joints. The use of a complex variable approach allows the development of simple and efficient algorithms to systematically formulate the equations. A procedure to solve the equations for several levels of normal loads in the friction joints is also presented. It only requires that systems of real linear equations be solved. Any degree of accuracy can be obtained by applying this procedure iteratively. In addition, a criterion is established for determining when joints transition from a slipping to a fully stuck condition.

Relevant computational issues are discussed, with emphasis on the interaction of the methodology with finite element programs. Selected examples are presented to illustrate applications of the methodology in practical problems as well as the most relevant features of the solution procedure. Some mathematical manipulations and more detailed descriptions of the algorithms are presented in Appendices.

2 Equations of Motion

We will consider a structural system consisting of several elastic substructures connected by friction interfaces and subjected to prescribed harmonic loads, as shown in Fig. 1. An appropriate finite element discretization of each substructure can be carried out shown schematically in Fig. 2 Thus, the system is represented as a set of elastic substructures with a finite number of degrees of freedom and connected by friction joints at some of their nodes. We will also consider that the normal loads in the friction joints are independent of the displacements and are given as a vector of positive constants times a positive scalar parameter, and that only displacements in the tangential direction can occur in those joints

A typical substructure has stiffness matrix K, mass matrix M, damping matrix C, and applied nodal loads Q, obtained by standard finite element techniques. Let X be the vector of displacements, which can be divided into two mutually exclusive vectors. X_1, corresponding to the degrees of freedom not connected to friction joints, and X_2, corresponding to the degrees of freedom connected to friction joints The stiffness, mass and damping matrices and the vector of nodal loads can be partitioned accordingly.

Newton's second law yields the following equations of motion for the substructure

$$M_{11}\ddot{X}_1 + M_{12}\ddot{X}_2 + C_{11}\dot{X}_1 + C_{12}\dot{X}_2 + K_{11}X_1 + K_{12}X_2 = Q_1 \tag{1}$$

2

$$M_{21}\ddot{X}_1 + M_{22}\ddot{X}_2 + C_{21}\dot{X}_1 + C_{22}\dot{X}_2 + K_{21}X_1 + K_{22}X_2 = Q_2 + F \qquad (2)$$

where dots denote derivatives with respect to time, and F is a vector containing the forces in the friction joints, with an appropriate sign that will be discussed later. These equations can be written for each substructure of the system, and are coupled by the friction forces, F.

The behavior of a friction joint can be described in terms of the relative displacement (difference between the displacements of the connected nodes) and the tangential force in the joint. Here, joints of Coulomb type are considered. This implies that when a joint, j, is sliding, its tangential force f_j must satisfy the condition $f_j = \mu_j N_j$, where μ_j and N_j are respectively the friction coefficient and the normal force in the joint. The sign of the force must be opposite to that of the relative velocity. These conditions hold until a change in the sign of the relative velocity occurs, causing the joint to become stuck or start sliding in the opposite direction. When the joint is locked its relative displacement remains constant and its tangential force is unknown, its value being a result of the analysis.

Exact analytical solutions for the total set of differential equations of motion are difficult to obtain, because it is necessary to know, at any time, which joints are sliding and which are stuck. This information, however, is part of the solution of the problem rather than part of the data. In general, for each joint, an unknown number of incursions in both conditions can take place during a period of vibration. Hence, any attempt to develop an exact solution in terms of piecewise linear solutions would lead to a problem which would have to be approached numerically and whose solution would require excessive computer resources.

Several well-known step-by-step time integration schemes can be used to solve approximately the equations of motion [1]. The main advantage of these procedures is that any number of slip-to-stick changes and vice versa can be considered without difficulty. However, for nonlinear steady-state problems the integration has to be carried out for a long time, enough to reach the periodic state, i. e., until the effect of the initial disturbances becomes negligible. Besides, to obtain accurate results in multiple-degree of freedom problems, the time step has to be several times smaller than the lowest relevant period of the system or any of the substructures. For these reasons numerical integration can become impractical even for systems with a moderate number of degrees of freedom.

3 Approximate Method of Solution

In view of the difficulties of obtaining analytical or numerical exact solutions, approximate methods have been used by several researchers [14, 6, 10]. The most widely used method is the so-called harmonic balance method which finds the best approximation of the response in the space of the harmonic functions with the same frequency as that of the excitation. This method is completely equivalent to the linearization technique proposed by Caughey [3]; its theoretical foundations have been thoroughly studied by Spanos and Iwan [15].

The following assumptions are made in the harmonic balance method:
1. All the responses are harmonic with the same frequency as that of the excitation forces;

2. The friction force in each joint has the same direction as the relative velocity in the joint, but opposite sign;

3. Only the first Fourier component of the friction force in each joint has a significant participation in the response of the system, i.e. the effects of higher components are negligible.

Another classical assumption is that the friction joints are always sliding, i.e., no stuck conditions are considered. Since in many practical cases the joints are only partially sliding, or even completely stuck, this assumption may lead to erroneous results. A criterion to determine the slip-to-stuck limiting loads is presented here, permitting the actual states of the joints to be considered correctly in the dynamic analysis.

3.1 Equations of Motion for a Typical Substructure

The harmonic excitation forces in the nodes of a typical substructure can be expressed as

$$q_j(t) = \hat{q}_j \exp(i\omega t) \, , \, j=1, ndf$$

where a caret ($\wedge$) denotes a complex quantity, t = time, $i = \sqrt{-1}$ and ndf = the number of degrees of freedom of the substructure.

According to assumptions (1) and (3) the elements $x_j(t)$ of the displacement vector and $f_j(t)$ of the friction forces vectors are also harmonic, i.e..

$$x_j(t) = \hat{x}_j \exp(i\omega t) \, , \, j=1, ndf$$

$$f_j(t) = \hat{f}_j \exp(i\omega t) \, , \, j=1, ndf$$

where $\hat{x}_j$ is an unknown complex constant. For a totally sliding joint, the friction force has the shape of an alternating square wave. Consequently, $\hat{f}_j$ is a complex constant with modulus $(4/\pi)\mu_j N_j$, where μ_j is the friction coefficient and N_j the normal load on joint j.

4

By substituting these expressions into (1) and (2) and dropping the factor exp(iωt), the following complex algebraic equations are obtained for the substructure:

$$(K_{11} - \omega^2 M_{11} + i\omega C_{11})\dot{X}_1 + (K_{12} - \omega^2 M_{12} + i\omega C_{12})\dot{X}_2 = \dot{Q}_1 \tag{3}$$

$$(K_{21} - \omega^2 M_{21} + i\omega C_{21})\dot{X}_1 + (K_{22} - \omega^2 M_{22} + i\omega C_{22})\dot{X}_2 = \dot{Q}_2 + \dot{F} \tag{4}$$

Define

$$\hat{k}_{ij} = K_{ij} - \omega^2 M_{ij} + i\omega C_{ij} \quad (i,j = 1,2)$$

$$\hat{r}^s = (\hat{k}_{22} - \hat{k}_{21}\hat{k}_{11}^{-1}\hat{k}_{12})^{-1} \tag{5}$$

$$\hat{z}^s = \hat{r}^s(\dot{Q}_2 - \hat{k}_{21}\hat{k}_{11}^{-1}\dot{Q}_1)$$

$$\hat{x}^s = \dot{X}_2$$

$$\hat{F}^s = \dot{F}$$

where the superscript s indicates that these matrices correspond to the s-th substructure. The matrix $\hat{k}_{ij}$ is called the impedance or dynamic stiffness matrix.

With the above definitions, (3) and (4) lead, after solving for $\dot{X}_2$, to

$$\hat{x}^s = \hat{z}^s + \hat{r}^s\hat{F}^s \tag{6}$$

which are equations relating the displacements of the degrees of freedom of substructure s to the tangential forces in its joints. A detailed derivation of these equations for two illustrative systems is presented in Appendix A. Vector $\hat{z}^s$ contains the part of the displacements produced by the external harmonic loads. $\hat{r}^s$ is called the compliance or dynamic flexibility matrix; its elements are displacements in the direction of the degrees of freedom associated with the joints, due to unit loads applied in the same directions. An efficient algorithm for the calculation of $\hat{z}^s$ and $\hat{r}^s$ is proposed in Appendix C.

Defining now $\dot{F}$ as the vector containing the friction forces in all the joints, the displacement of a generic degree of freedom j of the substructure s can be expressed as

$$\hat{x}_j^s = \hat{z}_j^s + \hat{r}_j^s\dot{F} \tag{7}$$

$\hat{x}_j^s$ and $\hat{z}_j^s$ are the corresponding elements of $\hat{x}^s$ and $\hat{z}^s$. $\hat{r}_j^s$ contains the corresponding terms of $\hat{r}^s$ and, in order to match the dimension of $\dot{F}$ contains zeros in the places corresponding to friction forces not related to the degree of freedom j. $\hat{r}_j^s$ also includes appropriate signs to account for the correct direction of the friction forces as it is discussed in the next section. The rewriting of expressions (6) into the form of (7) is illustrated in Appendix A.

5

3.2 Equations for the Complete System

We now derive the equations for a typical system, like the one depicted in Fig. 1. The first step is to define the relative displacements in the joints, as follows

$$\hat{d}_j = \hat{x}_k^m - \hat{x}_l^n \tag{8}$$

The superscript m can be assigned arbitrarily to any of the substructures connected by the joint j; n denotes the other connected substructure. The subscripts k and l denote, respectively, the degrees of freedom of substructures m and n that are connected to joint j. This step is illustrated in Appendix A.

Expression (8) means that, by definition, a positive relative velocity in joint j points from n to m. Therefore, according to assumption (2) at the beginning of this section, a positive friction force points from m to n. Consequently, this force has already the correct sign when acting on substructure m, and has to be affected by a negative sign when acting on substructure n. This rule is used when writing equations (7), as it is also illustrated in Appendix A. Replacing $\hat{x}_j^s(s=m,n; j=k,l)$ given in (7) into (8) we obtain

$$\hat{d}_j = (\hat{z}_k^m - \hat{z}_l^n) + (\hat{r}_k^m - \hat{r}_l^n)\hat{F}$$

One equation can be written for each degree of freedom in the friction interfaces obtaining the following system of complex algebraic equations

$$\hat{D} - \hat{R}\hat{F} = \hat{Z} \tag{9}$$

for the relative displacements in the friction joints in terms of the corresponding friction forces and known displacements $\hat{Z}$. Details of the derivation of $\hat{R}$ and $\hat{Z}$ for illustrative systems are included in Appendix A.

The number of unknowns in these equations is twice the number of equations. To complete the formulation, it is necessary to use the constitutive relationships between the joint displacements $\hat{D}$ and forces $\hat{F}$. Within the frame of the assumptions considered in this work, the relative displacement in a generic joint j is

$$(\hat{x}_k^m - \hat{x}_l^n)\exp(i\omega t) = \hat{d}_j \exp(i\omega t) \tag{10}$$

$\hat{d}_j$ is a complex constant that can be expressed as $d_j \exp(i\theta_j)$, where d_j and θ_j are the corresponding amplitude and phase angle.

By differentiation of (10) the relative velocity can be written as $i\omega \hat{d}_j \exp(i\omega t)$. Recalling that the friction force in joint j is expressed as $f_j(t) = \hat{f}_j \exp(i\omega t)$, and that this force is opposed to the relative velocity, we conclude that complex constant $\hat{f}$ has the form $\hat{f}_j \exp(i\theta_j)$, where f_j is the (real) amplitude of the force. Defining $a_j = d_j f_j$ we have

$$\hat{d}_j = i(d_j/f_j)\hat{f}_j = ia_j\hat{f}_j \qquad (11)$$

The ratio a_j is always positive and can vary between zero and infinity. Both limiting values lead to special linear problems. a_j equal to zero means that there is no relative displacement in the j-th joint. On the other hand, a_j equal to infinity corresponds to the case of no normal force (and as a consequence, no friction force) in the joint.

Equation (9) can be now written as

$$[iA - \hat{R}]\hat{F} = \dot{Z} \qquad (12)$$

where A is a real diagonal matrix with entries a_j.

For prescribed values of A, (12) is a linear system of complex equations for the friction forces $\dot{F}$ that can be solved directly. We are, however, interested in solutions for prescribed normal forces in the joints, i.e., for prescribed amplitudes of $\dot{F}$ and not of A . In this case, a_j cannot be calculated directly because the values of d_j are still unknown. This problem is addressed in the next section, as part of the proposed solution methodology.

4 An Efficient Solution Procedure

4.1 General

In the cases of interest for this report, the normal loads in the joints are prescribed as a vector of real constants times a scalar parameter N, i. e., as

$$\left\langle \begin{array}{c} N_1 \\ N_2 \\ \\ \vdots \\ \\ N_n \end{array} \right\rangle = N \left\langle \begin{array}{c} e_1 \\ e_2 \\ \\ \\ \\ e_n \end{array} \right\rangle \qquad (13)$$

In practical design problems, it is desired to find the solution for different values of N, and, eventually, to calculate the N for which the response controlling the design (displacement, stress, etc) is a minimum. This is the optimum value of the parameter N

If the joint j, with friction coefficient μ_j, is sliding, the amplitude of the friction force in that joint is $f_j = (4/\pi)\mu_j N_j$. In this joint, the relative displacement has an unknown amplitude d_j

7

In general, for a given value of N, some joints will be sliding, and the rest will be locked. There are two limiting conditions; the first one occurs for high values of normal forces, preventing any slip of the joints. In this case the governing equation (9) reduces to $\dot{R}\,\dot{F} = -\dot{Z}$, which can be solved directly. The other limiting case corresponds to no normal forces (N = 0) and, consequently. no friction forces in the joints. All the joints are slipping, and the relative displacement $\dot{D}$ are equal to $\dot{Z}$.

It can be easily shown that Gaussian elimination of the equations corresponding to the locked joints (using the condition that the relative displacements are zero) yields a reduced system of equations of the same form as (9), but containing only terms related to the sliding joints. As pointed out before, it cannot be asserted that the amplitude of all of the forces is $f_j = (4/\pi)\mu_j N_j$, because this is acceptable only for joints that are at least partially sliding. For a locked joint the value of f_j is completely unknown and must be determined as part of the solution.

4.2 The Basic Step

The solution algorithm developed in this work is summarized in this section. It essentially consists of finding first the solution when all the joints are slipping, and then, using perturbations, progressively calculating the solutions as the normal loads are increased. The basic step of the algorithm is presented next.

Equation (9) can be written as

$$\dot{F} + \dot{K}\dot{D} = \dot{F}_0 \tag{14}$$

where $\dot{K} = -\dot{R}^{-1}$ and $\dot{F}_0 = \dot{K}\dot{Z}$. Assume that solution vectors $\dot{F}$ and $\dot{D}$ for normal forces defined by $N = N_0$ are known. The solution for another, close, value of $N = N_0 + \Delta N$ is desired. Let $\dot{F}_1$ and $\dot{D}_1$ denote the new solution vectors, and define $\Delta \dot{F}$ and $\Delta \dot{D}$ so that

$$\dot{F}_1 = \dot{F} + \Delta\dot{F} \text{ and } \dot{D}_1 = \dot{D} + \Delta\dot{D} \tag{15}$$

Since $\dot{F}$ and $\dot{D}$ satisfy (14) we can write

$$\Delta\dot{F} + \dot{K}\Delta\dot{D} = 0 \tag{16}$$

Note that this is an exact relationship between the complex increments of friction forces and relative displacements. Recalling that the elements of $\dot{F}$ and $\dot{D}$ in the known solution are $\hat{d}_j = d_j\exp(i\theta_j)$ and $\hat{f}_j = -if_j\exp(i\theta_j)$, the increments can be approximated by truncated Taylor's series expansions as follows

$$\Delta\hat{d}_j = \exp(i\theta_j)\Delta d_j + i\hat{d}_j\Delta\theta_j$$

$$\Delta\hat{f}_j = -i\exp(i\theta_j)\Delta f_j + \hat{f}_j\Delta\theta_j$$

Substitution into (16), after algebraic manipulations, yields the following system of linear equations for the increments of amplitudes and phase angles of the relative displacements

8

$$B_i \Delta d + B_r H \Delta \theta = \Delta f \tag{17}$$

$$B_r \Delta d + (G - B_i H) \Delta \theta = 0 \tag{18}$$

where B_r and B_i are the real and imaginary parts of the complex matrix product $\dot{U}^* K \dot{U}$. $\dot{U}$ is a unit complex diagonal matrix with nonzero elements $\hat{u}_{jj} = \exp(i\theta_j)$. $\dot{U}^*$ is the complex conjugate of $\dot{U}$. Δd and $\Delta \theta$ are real unknown vectors of amplitudes and phase angles of the relative displacements. H and G are real diagonal matrices with nonzero elements d_j and f_j, respectively. ΔF is the known vector of increments in the amplitudes of the friction forces. Note that the matrices defining the coefficients of the system (17) and (18), which are used to estimate the solution each time N is increased, are expressed in terms of the known solution.

Solving for Δd and $\Delta \theta$ we have an approximation for ΔF that can be used to compute $\dot{F}_1$ and $\dot{D}_1$. The accuracy of this approximate solution can be verified by computing $\dot{F}_2 = \dot{F}_0 - \dot{K} \dot{D}_1$, and comparing $\dot{F}_2$ with $\dot{F}_1$. If the comparison is not satisfactory, it is possible to compute a new starting solution that satisfies (14) calculating the ratios $a_j = d_j / f_j$ with $\dot{D}_1$ and the desired values of the amplitudes of the tangential forces. Introducing the estimated a_j into (12) another vector of forces, $\dot{F}_3$, is obtained. In general, $\dot{F}_3$ will be different from $\dot{F}_1$. The amplitudes of the elements of the complex vector $(\dot{F}_3 - \dot{F}_1)$ can be taken as a new vector Δf in (17) using $\dot{F}_3$ to compute the coefficients of equations (17) and (18). The steps can be repeated iteratively in the following manner until a desired accuracy is reached.

1. Solve the system under the assumption that all the joints are slipping, and define the initial values of f_j, f_j^0.

2. Increase the value of μN.

    2.1 Compute Δf, vector of increments of the amplitudes of the tangential forces, $\Delta f_j = f_j^1 - f_j^0$.

    2.2 Compute Δd, vector of increments of the amplitudes of the relative displacements.

    2.3 Calculate the new relative displacements, $d_j^1 = d_j^0 + \Delta d_j$, and the ratios $a_j = d_j^1 / f_j^1$.

    2.4 Solve equations (12) and compute f_j^2.

    2.5 If, within some acceptable tolerance, $f_j^2 = f_j^1$ continue with 2.6
    - If not, set $f_j^0 = f_j^2$ and start 2.1 again.

9

2.6 Verify that all the joints are actually slipping, i.e. if all d_j^1
are positive. Yes, define $f_j^0 = f_j^2$ and consider the next
value of μN (go to 2). No, eliminate equations corresponding to the
locked joints (negative amplitudes) and start 2.1 again.

3. The procedure finishes when all the joints are locked.

4.3 Slip-to-Stick Transitions

In the previous section it has been assumed that all the joints are slipping. This assumption is certainly valid when the joint normal loads are small but must be checked as N increases. As N increases, the amplitudes of the relative joint motions decrease. When the calculated amplitude of a joint's relative motion becomes zero (or negative) that joint is considered locked for subsequent analyses, the amplitude of its relative motion is set identically equal to zero and the associated degree of freedom may be eliminated from the set of nonlinear algebraic equations. Thus, the number of nonlinear equations that must be solved becomes progressively smaller as the normal loads are increased and the joints lock. When a joint is considered locked, the force transmitted by friction through it may be calculated as a result of the analysis. The joint is actually locked if the amplitude of the force is smaller than μNe_j. The slipping and stuck models are then said to be compatible and there is no transition region where the simple harmonic assumption breaks down.

In solving the numerical example described in the next section, it was found that convergence to negative values for the amplitudes of the relative displacements is possible. Examining equations (18), it can be observed that no restrictions are imposed on the values of the increments of the relative displacements Δd in order to prevent this condition. The physical interpretation of a negative amplitude is that the corresponding joint is already locked and this condition can be used to eliminate that joint from the system of equations. For this reason, it is important to have an accurate criterion for establishing at what normal loads each joint becomes stuck. Such a criterion can be formalized in the following manner.

We start with the solution for $\mu N = \mu N_0$, for which all the joints under consideration are sliding. The friction forces and the relative displacements are $f_{0j} = (4/\pi)e_j \mu N_0$ and d_{0j}, respectively. The desired solution corresponds to an unknown value of μN for which $f_j = (4/\pi)e_j \mu N$. Therefore, the differences in the amplitudes of the friction forces are

$$\Delta f_j = (4/\pi)(f_j - f_{0j}) = (4/\pi)(e_j)(\mu N - \mu N_0) = (4/\pi)(e_j)(\Delta \mu N) \tag{19}$$

Solving (17)-(18) for a unit increment in μN, i.e. for $\Delta f_j = 4 \pi e_j$, we obtain increments Δd_j for the relative displacements. The total values are

10

$$d_j = d_{0j} + \Delta\mu N \Delta d_j \tag{20}$$

For $\Delta\mu N$ yielding $d_j = 0$ the joint j will become locked. Applying this condition to each joint, n values of μN are obtained, where n is the number of joints under consideration. The key result is the smallest value of normal load increment for which lock up occurs since it is the corresponding joint which will be the first to stop slipping.

5 Computational Issues

The several steps of the methodology proposed in this work are suitable for incorporation in computer codes. Detailed rules to carry out automatically such steps are provided in this section, including the required data structures and some particular numerical algorithms. All the matrices and vectors used in this section are complex; however the carets (^) used in remainder of the text to distinguish these quantities form the real ones have been omitted, to obtain a more readable text.

The calculation of stiffness, mass and damping matrices requires only standard finite element techniques, whose efficiency and computer implementation are widely discussed in the technical literature on the subject and will not be discussed here. This section deals with steps of the methodology that are not direct applications of finite element procedures.

5.1 Compliance Matrices of Substructures

The starting step of the formulation is Eq. (6). The reduced compliance matrix r^s of the substructure s of this equation is defined in Eq. (5) as the inverse of the reduced impedance matrix, namely as

$$r^s = (K_{22} - K_{21}K_{11}^{-1}K_{12})^{-1}$$

The vector z^s is also defined as a reduced displacement vector, in terms of the inverse of K_{11}. The impedance matrix of a substructure can be calculated with any finite element code. With this, the required matrix partitions, inversions and products could be performed directly. However, it is more efficient to proceed as follows:

    a. Compute the total impedance matrix of the substructure. K

    b. Solve $K y = Q$ (the load vector, Q, is known).

    c. Select the terms of y corresponding to degrees of freedom connected to
       friction joints. This constitutes the reduced vector z

11

d. For each degree of freedom, j, connected to a friction joint:

   d.1 Form a unit load vector, q, with all its terms equal to zero except
   the j-th term, which is equal to 1.

   d.2 Solve $K y = q$.

   d.3 The j-th column of r is formed by the terms of y corresponding
   to degrees of freedom connected to friction joints.

5.2 Automatic Generation of the System's Equations

A detailed derivation of the equations relating the relative displacements and the tangential forces in the joints for two illustrative systems is presented in Appendix A. A simple algorithm for the automatic generation of these equations for any given system, starting from the reduced compliance and displacements matrices, r^s and z^s, of the substructures forming the system, consists of the following steps:

a. Assign an order number s to each substructure and an order number j to each
   friction interface.

b. Recall that the r^s matrix of substructure s is reduced to its degrees of
   freedom connected to friction interfaces. Consider r^s partitioned
   according to those interfaces. Let p be the number of partitions. A
   typical term of r^s is r^s_{uv}, $u,v = 1,p$

   A similar partition for vector z^s results in a typical element z^s_u, $u = 1,p$

c. For each friction interface define, arbitrarily, a direction for the relative
   displacements, i. e., a "starting" reference substructure, m, and an "ending"
   substructure, n. The relative displacement in joint j is given by

   $$d_j = x^m_i - x^n_i$$

   where x^m_i is the total displacement of substructure m in the direction
   of its degrees of freedom connected to the joint, i. A similar
   definition applies to x^n_i

d. Form an incidence vector, V^s, for each substructure s, containing
   the order numbers of the interfaces to which substructure s is connected

12

Observe the following rules:

 d.1 the size of the vector is p;

 d.2 the order of the incidences agrees with that used when computing r^s;

 d.3 the sign of an incidence is positive if s is a starting substructure
  for the corresponding interface and negative if the substructure is
  an ending one.

e. Form the system matrix R by adding the contributions of each
 substructure, as follows:

 e.1 the size of the matrix is equal to the total number of friction joints;

 e.2 add p^2 terms of the form r_{uv}^s;

 e.3 define iu = u-th term of the incidences vector V^s, and iv = v-th
  term of the incidence vector V^s;

 e.4 r_{uv} is added to $R_{iu,iv}$, with the sign of the product (iu)(iv).

f. Form the system displacements vector Z, by adding the term z_u^s
 to Z_{iu}, with the sign of iu.

Note the similarity between these rules and those to form the stiffness matrix of a structure from the element matrices in the Direct Stiffness Method . All the advantages of this method, such as sparsity, banded or skyline shapes, etc. are in fact preserved

The proposed algorithms have been applied to the illustrative systems depicted in Figures 10 and 11 in Appendix C. Additional rules are presented there to include some particular cases.

6 Numerical results

To verify the accuracy and applicability of the methodology, the solution of the one-joint problem depicted in Fig. 3 was computed over a range of values of the system parameters using the approximate method and the results compared with exact solutions. The exact solution was developed in [2] by exploiting the piecewise linearity of the differential equation, i e , when the joint is slipping the friction force is constant and the solution can be represented by one set of harmonic functions with unknown

coefficients, and when the joint is stuck the system is also linear and can be represented by another set of harmonic functions with unknown coefficients. The coefficients are calculated along with the time at which transition occurs between slipping and sticking by forcing the solutions to satisfy the appropriate continuity and periodicity conditions. In general, the results from the approximate procedure compared quite well with exact solutions [2]. Representative results are shown in Table 1 for $M_1 = M_2 = 0.5$, $K_1 = 0.25$, $K_2 = 0.75$, $Q = 1.0$, $\alpha = \beta = 0.0$, and $C_1 = C_2 = 1$ percent of critical. The two cases shown in the table are for excitations frequencies of $\omega = 0.707$ and $\omega = 1.0$. These frequencies are particularly interesting since the first corresponds to the resonant frequency that the system would have if the damper were slipping all the time, while the second is the resonant frequency of the system when the damper is stuck all the time. Consequently, these two frequencies turn out to be the frequencies of most interest in the limit for either very large or small excitations, respectively.

Part (a) of the table shows exact and approximate results for $\omega = 0.707$. As is indicated by the table the approximate method provides results which are in close agreement with the corresponding exact values. Part (b) of the table shows exact and approximate results for $\omega = 1.0$. In this case the approximate procedure was less accurate, but still adequately predicted the absolute displacement of the masses. The absolute displacement of the masses were of comparable magnitude; consequently, small errors in their values resulted in relatively large percentage errors in the relative displacement as it approached zero. This is a limitation of the approximation caused by the fact that if slip occurs the Fourier coefficient of the friction force is taken to be $4/\pi$, independently of the amplitude of the relative motion. In fact, this value must converge to unity as the relative motion goes to zero and it is this discrepancy that induces the errors previously cited. A number of procedures were tried for approximating this transition of the Fourier coefficient from $4/\pi$ to 1 as the amplitude of the relative motion went to zero. In general, none of the approaches worked (on the average after taking all frequencies of excitation into consideration) any better than the simple one utilized here of setting the Fourier coefficient equal to $4/\pi$ when the joint slips.

In summary the approximate approach used in this report proved to be a relatively accurate method for calculating the absolute and relative motions of the vibrating masses except for small relative motions at an excitation frequency near the natural frequency of the locked system. Under these conditions, it adequately predicted the absolute motion of the masses and qualitatively predicted the correct trends, but yielded significant percentage errors in values of relative motion between the masses. This is a limitation of the approach that should be taken into consideration in its use.

To demonstrate the applicability of the methodology in design problems we have analyzed the system

14

with two substructures and two friction joints shown in Fig. 4. Plate finite elements (including only bending deformations) were used to calculate the stiffness and mass properties of each substructure and structural damping was set at 1 percent of critical damping. The stiffness matrices are also presented in Fig. 4. External loads amplitudes $Q_1 = 1$ and $Q_2 = 1$ were considered. The normal forces in the friction joints are defined by $e_1 = 1$ and $e_2 = 2$.

The natural frequencies and modes of vibrations for the system with the joints locked, and for substructure 1 isolated were calculated (substructure 2 was considered massless). The mode shapes for the isolated substructure are shown in Fig. 4. The mode shapes for the total system are similar, but correspond to higher frequencies. In both cases, the first mode is flexural, and the second one, torsional.

In the dynamic analysis the excitation frequency was varied between 400 and 1500 rad/sec to include the four possible resonant conditions (see values below). Several values of the normal force in the joints were considered.

Results are summarized in Figs. 5 through 9. In Fig. 5 the maximum horizontal displacement of substructure 1 in the joint 1 is presented as a function of the excitation frequency. The first peak in Fig. 5 corresponds to the first natural frequency of substructure 1 ($\omega = 586$ rad/sec) and occurs when there are no forces, and consequently no energy dissipation, in the joint. If the normal forces increase, the response for that particular frequency decreases quickly. However, for frequencies close to the first natural frequency of the complete system ($\omega = 702$ rad/sec) the response increases very rapidly, and a second peak is reached. This peak has its maximum value when the normal forces are high enough to keep the joints locked, preventing energy dissipation by friction. The variation of the response around these frequencies can be more clearly appreciated in Fig. 6, where the first part of Fig. 5 is repeated with an enlarged frequency axis. Peak responses also occur for the corresponding second natural frequencies ($\omega = 1215$ and 1412 rad/sec), but their values are only 23% of the former ones.

Fig. 7 shows values of the normal forces for which a change from the stuck to the sliding condition (or vice versa) occurs in each friction joint. For a prescribed frequency, a joint is locked for normal forces that e· r ·ed the value given in the corresponding curve. For given normal loads, a horizontal line can be drawn in Fig. 6 to find the limiting frequencies for which each joint is either always stuck or always sliding. The slip-to-stuck curve has a peak at $\omega = 702$, the first resonant frequency when the joints are locked. The reason is that the lar· ·st tangential forces in the joints under harmonic excitation occur for this resonant condition, requirii   e maximum normal loads to prevent slipping. The slip-to-stuck curve for a wider range of frequencies is presented in Fig. 8, where it can be appreciated that a second peak exists for the second (torsional) resonant frequency of the locked system.

15

Results presented in Fig. 9 can be useful for design purposes. This figure shows the maximum value, x_{1max}, of the displacement at node 1, as a function of the parameter μN defining the normal forces in the joints. It was obtained by considering all the possible values of the excitation frequency, i. e., by taking the peak values of the response curves of Fig. 5. The optimum value of μN is the one that gives the minimum value of x_{1max} (0.6 in this case). A similar curve was developed for the displacement in node 2, and the same optimum value of μN was obtained. Curves corresponding to any other response of interest can be easily constructed. Naturally, it is highly desirable to design the friction joints to have values of the normal forces close to the optimum ones.

7 Conclusions

A simple methodology for analyzing the steady-state vibrations of linear structures containing friction interfaces was presented. The numerical problem is reduced to the solution of systems of linear algebraic equations. Well-known, efficient algorithms can be used for this purpose. The main hypotheses are that the response is harmonic with the same period as that of the excitation, and that only the first Fourier components of the friction forces have a significant participation in the dynamic response. It can be noted that, for the simple Coulomb model of friction used here, the Fourier series for the nonlinear forces would contain only odd integer multiples of the fundamental frequency, and that the amplitudes of the terms decrease at least as fast as their frequencies increase. Consequently, we would expect relatively minor contributions from the higher order harmonics that have been neglected. As a result, we expect the solution procedures presented here to be reasonably accurate in most situations.

Within the frame of the above assumptions, the complex variable approach presented here is an efficient and systematic tool which can be utilized to derive the equations governing the motion of the friction joints in terms of their relative displacements and tangential forces. In fact, it is possible to formulate the equations in a similar manner to the direct stiffness method, taking advantage of the topological and storage procedures devised for such a method.

The comparison of numerical results for the single-joint problem of Fig 3 shows that the approximate methodology can yield very good estimates of the exact results. The major discrepancies occur when the joints are only partially sliding, because in these cases the first Fourier coefficients of the friction forces are closer to unity and not to $4/\pi$. The errors could be reduced by using some rules to calculate the Fourier coefficient as a function of the normal forces in the joints. These rules can be easily incorporated in the methodology; however, their general applicability must be carefully verified first.

The linearization concepts proposed in this work can be used for systems with friction interfaces

obeying different constitutive laws. In general, assuming that the response is harmonic, the differential equations can be transformed into a system of algebraic nonlinear equations relating relative displacements and friction forces in the joints. The equations can be linearized by considering truncated Taylor expansions in terms of the increments of the unknowns.

A criterion to determine the slip-to-stuck transitions in the joints is required to correctly formulate the problem under study, whatever method of solution is employed. It can be appreciated in Table 1 that it is mathematically possible to obtain negative amplitudes for the relative displacements in the joints. Similar results were obtained in the two-joint problem. Physically, this would correspond to friction forces with the same, not opposite, direction as the relative velocities. In reality, the joints are locked, and that physical fact must be incorporated into any solution procedure one may use to calculate the response for high joint normal loads.

The inclusion of possible locked joints allows a direct extension of the methodology to systems comprising substructures continuously connected, like the bladed disks of turbine engines or similar circumferentially periodic structures. The continuous interfaces can be treated as friction interfaces with the joints always locked.

The methodology presented here constitutes a good compromise between numerical effort and accuracy. This is particularly true when a large number of cases have to be solved. For instance, the derivation of optimization curves, as that depicted in Fig 9, requires solutions for a wide range of frequencies, for each set of normal load values. In this case, the methodology takes advantage of the already known solutions to find additional ones. In addition, if an exact solution is required, the approximate results could be used as initial conditions to solve the differential equations of motion using finite difference methods. This would significantly reduce the time for which integration has to be carried out, since the initial guess would be close to the steady-state solution.

References

[1] Bathe, K-J. and Wilson, E.L.
     Numerical Methods in Finite Element Analysis.
     Prentice Hall, Englewood Cliffs, New Jersey, 1976.

[2] Bazan-Zurita, E., Menq, C-H., Bielak, J and Griffin, J H.
     Steady-State Vibrations of a Two-Body System with a Frictional Interface. Department of Civil
     Engineering, Carnegie Mellon University, Pittsburgh, PA, 1986.

[3] Caughey, T.K.
     Sinusoidal excitation of a system with bilinear hysteresis.
     ASME, Journal of Applied Mechanics 27 640-643, 1960.

[4]   Menq, C-H. and Griffin, J.H.
      A Comparison of Transient and Stedy State Finite Element Analyses of Forced Response of a
      Frictionally Damped Beam.
      ASME 83-DET-24, *presented at the Design and Production Engineering Technical Conference,*
      Sep. 11-14, 1983.

[5]   Den Hartog, J.P.
      Forced Vibrations with Combined Coulomb and Viscous Friction.
      Trans. ASME AMP-53-9, pp. 107-115, 1931

[6]   Dominic, R.J., Graf, P., and Raju, B.B.
      Analytical and Experimental Investigation of Turbine Blade Damping.
      University of Dayton Publication, UDR-TR-82-39, August 1982.

[7]   Griffin, J.H.
      Friction Damping of Resonant Stresses in Gas Turbine Airfoils
      Asme Journal of Engineering for Power 102-329-333, April 1980

[8]   Hurty, W.C.
      Dynamic Analysis of Structural Systems Using Component Modes.
      AIAA Journal 3(4) 678-685, April 1965

[9]   Mahalingam, S.
      The Synthesis of Vibrating Systems by Use of Internal Harmonic Receptances.
      Journal of Sound and Vibration 40(3) 337 350, 1975.

[10] Muszynska, A. Jones, D i G , Lagnese T , and Whitford, L
      On Nonlinear Response of Multiple Blade Systems.
      Shock and Vibration Bulletin 51(3) 88 110, May 1981

[11] Plunkett, R
      Friction Damping on Damping Applications for Vibration Control
      AMD 38, 1980

[12] Przemieniecki, J S
      Theory of Matrix Structural Analysis
      McGraw-Hill, New York, 1968

[13] Sinha, A. and Griffin, J.H.
      Friction Damping of Flutter in Gas Turbine Engine Airfoils. *AIAA Journal of Aircraft* 20(4):372-376,
      April 1983

[14] Soni, M.L. and Bogner, F.K.
      Finite Element Vibration Analysis of Damped Structures
      AIAA Journal, Vol. 10, No. 8, pp. 700 707 20(8) 700 707, 1982

[15] Spanos, P-T D and Iwan, W.D.
      On the existence and Uniqueness of Solutions Generated by Equivalent Linearization
      Int. J. Non Linear Mechanics 13 71-78, 1978

[16] Srinivasan, A.V , Lionberger, S.R. and Brown, K.W
      Dynamic Analysis of an Assembly of Shrouded Blades Using Component Modes
      ASME Journal of Mechanical Design] 100 520-527, July 1978

[17] Srinivasan A V , Cutts, D.G., and Shidhar, S
      Turbojet Engine Blade Damping
      NASA Contract Report 165406, July 1981

Nomenclature

A diagonal matrix with entries a_j

a_j ratio d_j/f_j

B_i imaginary part of $\dot{U}^*K\dot{U}$

B_r real part of $\dot{U}^*K\dot{U}$

C damping matrix

D vector of relative displacements

d_j relative displacement in joint j

e_j factor for normal force in joint j

F vector of friction forces

f_j friction force in joint j

G diagonal matrix with entries f_j

H diagonal matrix with entries d_j

i unit of imaginary numbers

K stiffness matrix

M mass matrix

N parameter defining normal forces

N_j normal force in joint j

Q vector of applied nodal forces

q_j load applied at node j

R reduced flexibility matrix

r condensed flexibility matrix

t time

U complex unit diagonal matrix

X vector of total displacements

x_j total displacement of node j

Z reduced vector of displacements

z condensed vector of displacements

α ratio of force amplitudes

β phase angle

Δ increment of

μ friction coefficient

θ vector of phase angles

θ_j phase angle in joint j

ω excitation frequency
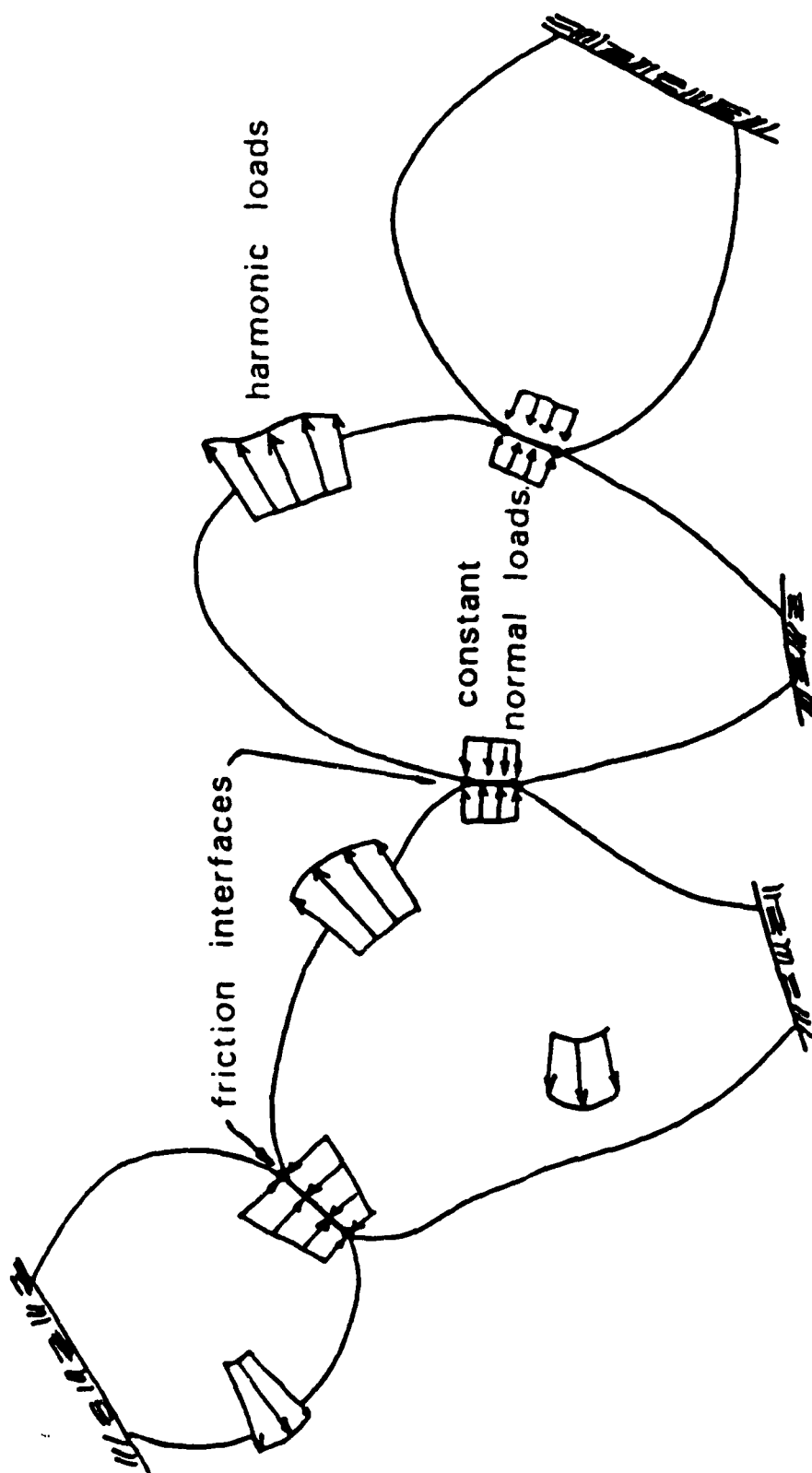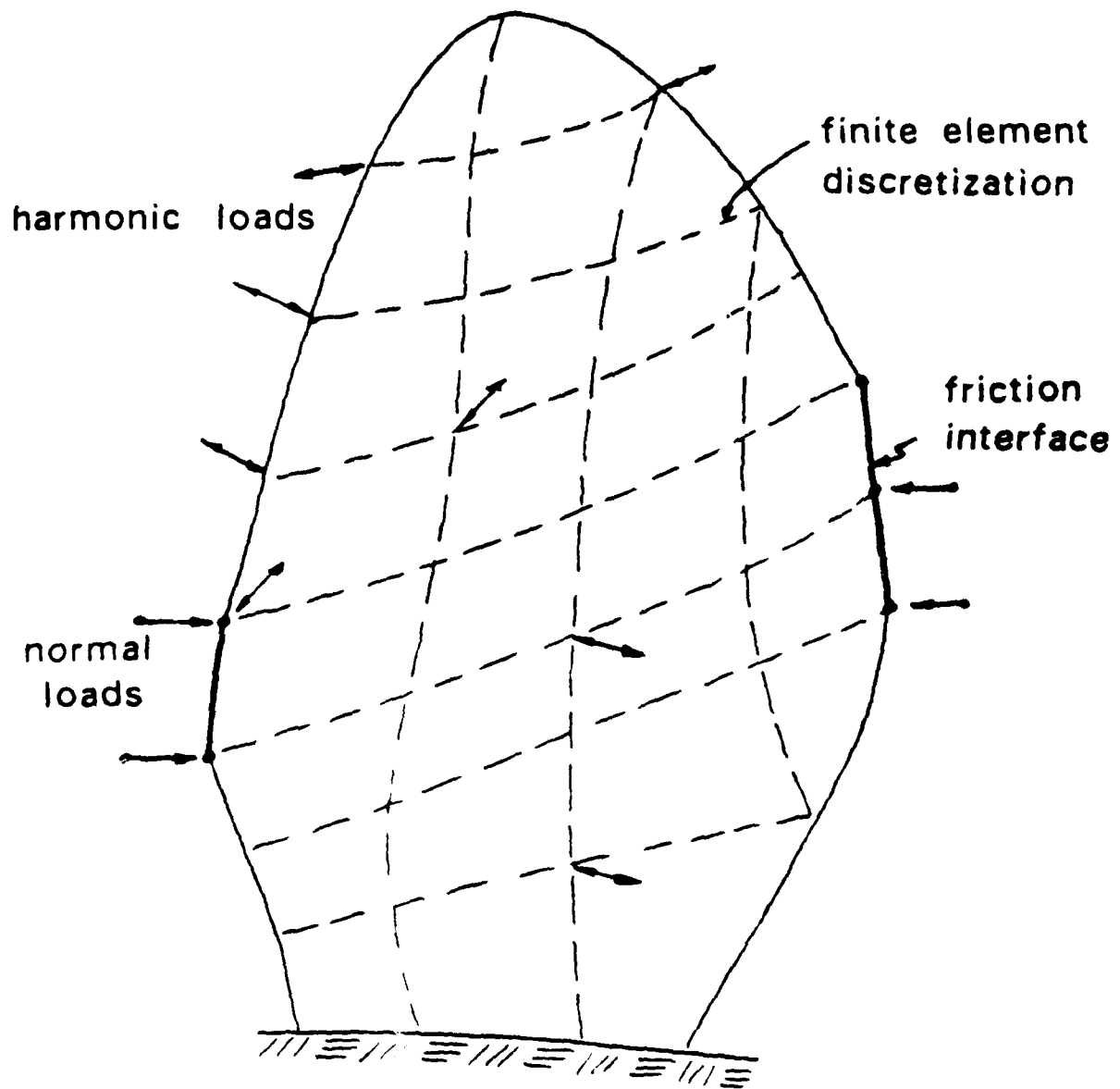
A caret (^) denotes a complex quantity.

Figure 1: System of Elastic Substructures Connected by Friction Interfaces

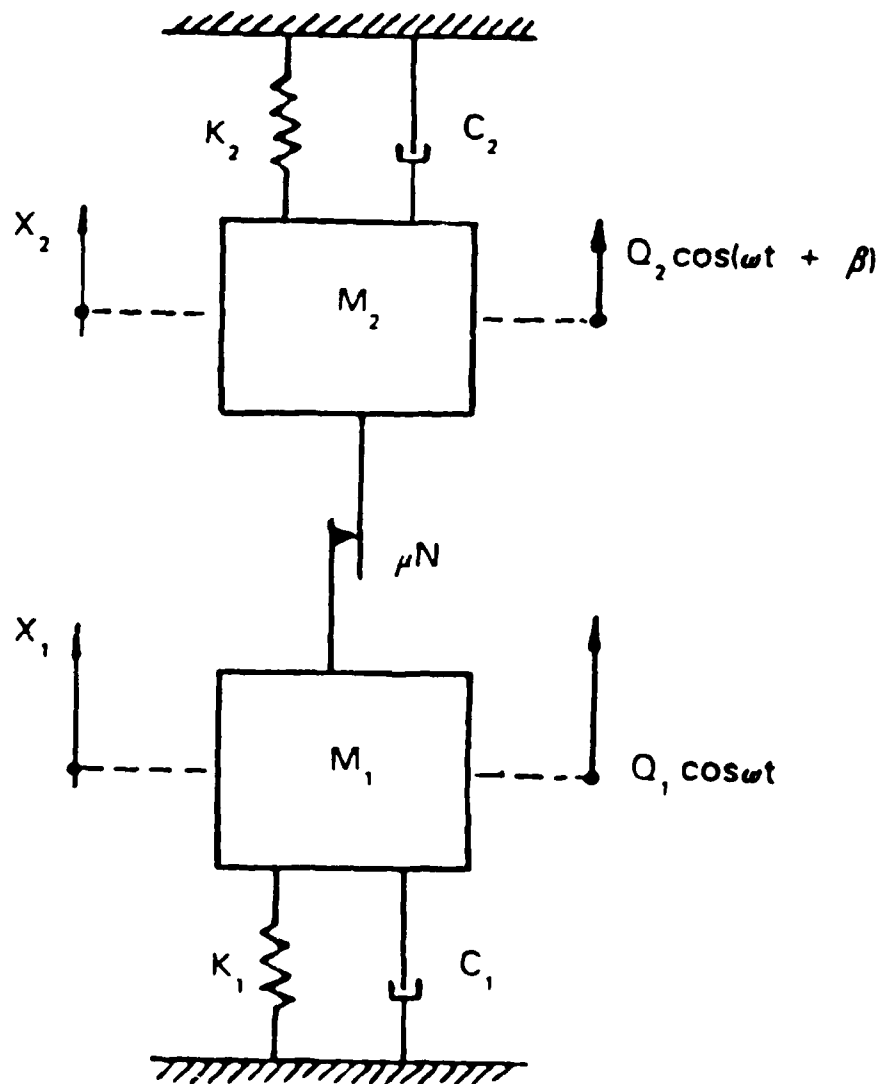**Figure 2:** Finite Element Model of a Substructure
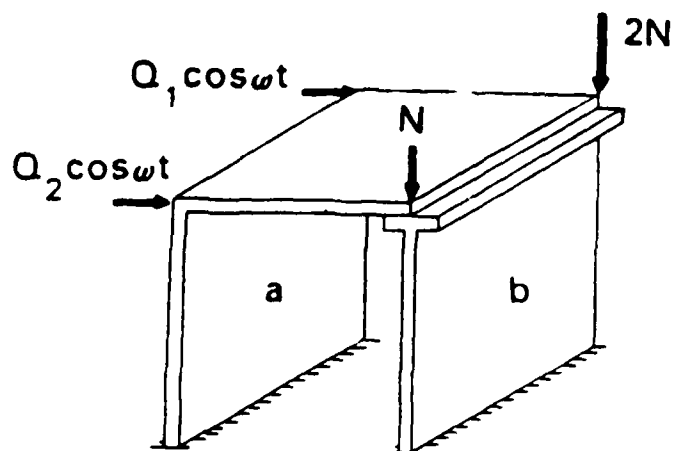
Figure 3:   Two-Body System with a Frictional Interface

$$K_a = \begin{bmatrix} 910.02 & -567.16 \\ -567.16 & 910.02 \end{bmatrix}$$

$$K_b = \begin{bmatrix} 333.33 & -183.33 \\ -183.33 & 333.33 \end{bmatrix}$$

$$M_1 = M_2 = 0.001$$
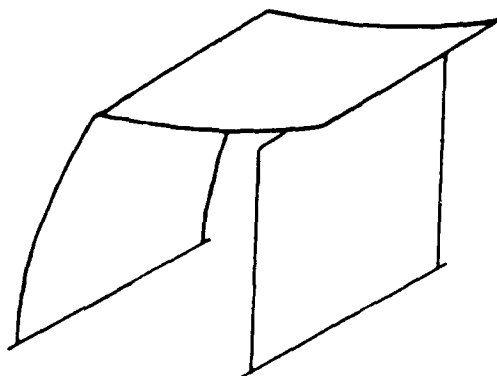
flexural vibration mode   torsional vibration mode
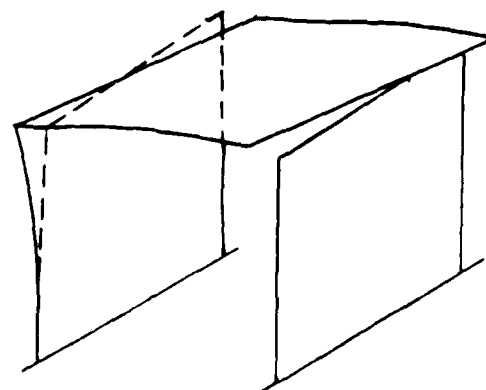
Figure 4:   Two-Joint Plate System
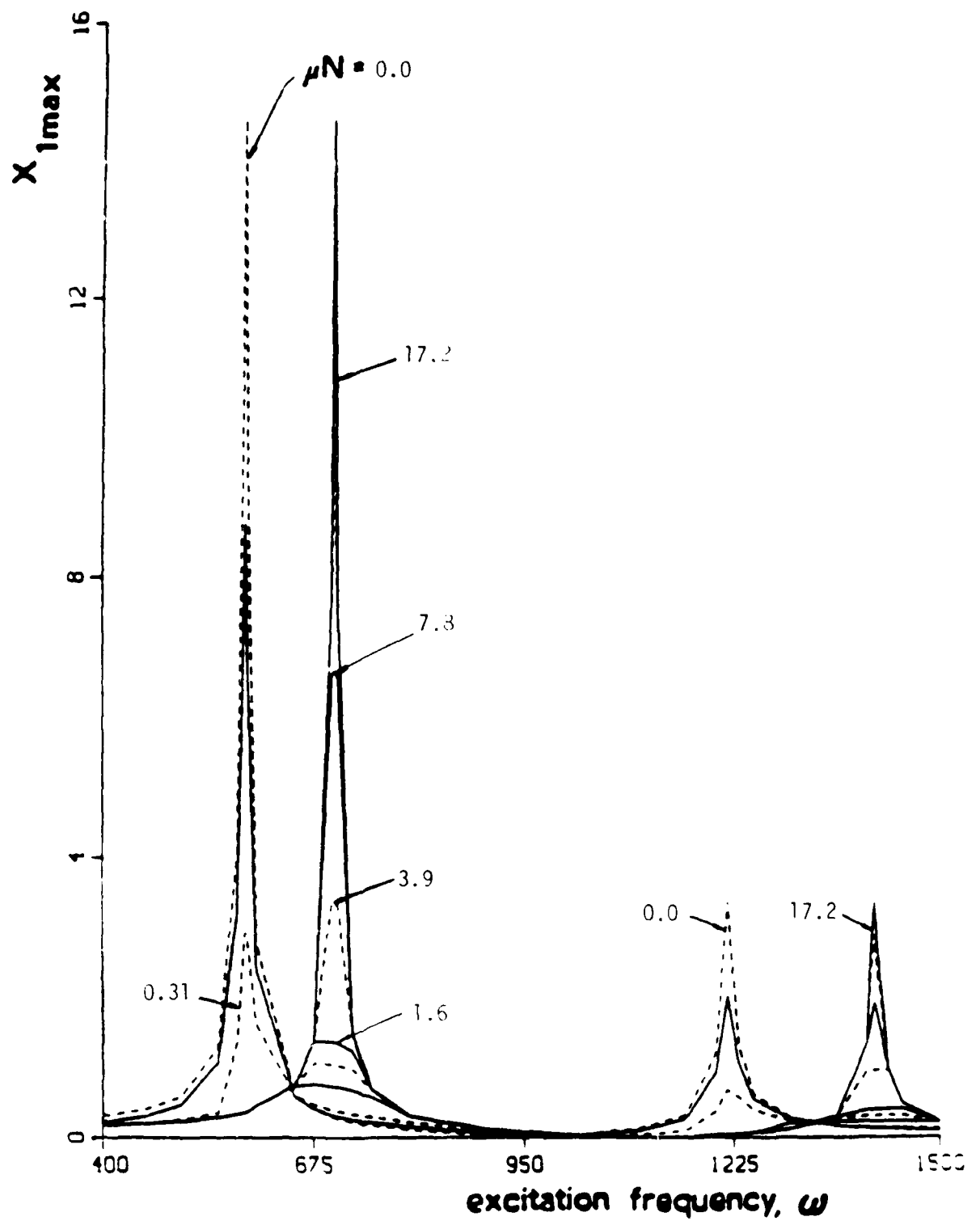
Figure 5: Maximum Response Curve for System of Fig. 4

Figure 6: Maximum Response Curve (enlarged) for System of Fig. 4

26

Figure 7: Slip-to-Stuck Transitions for System of Fig. 4
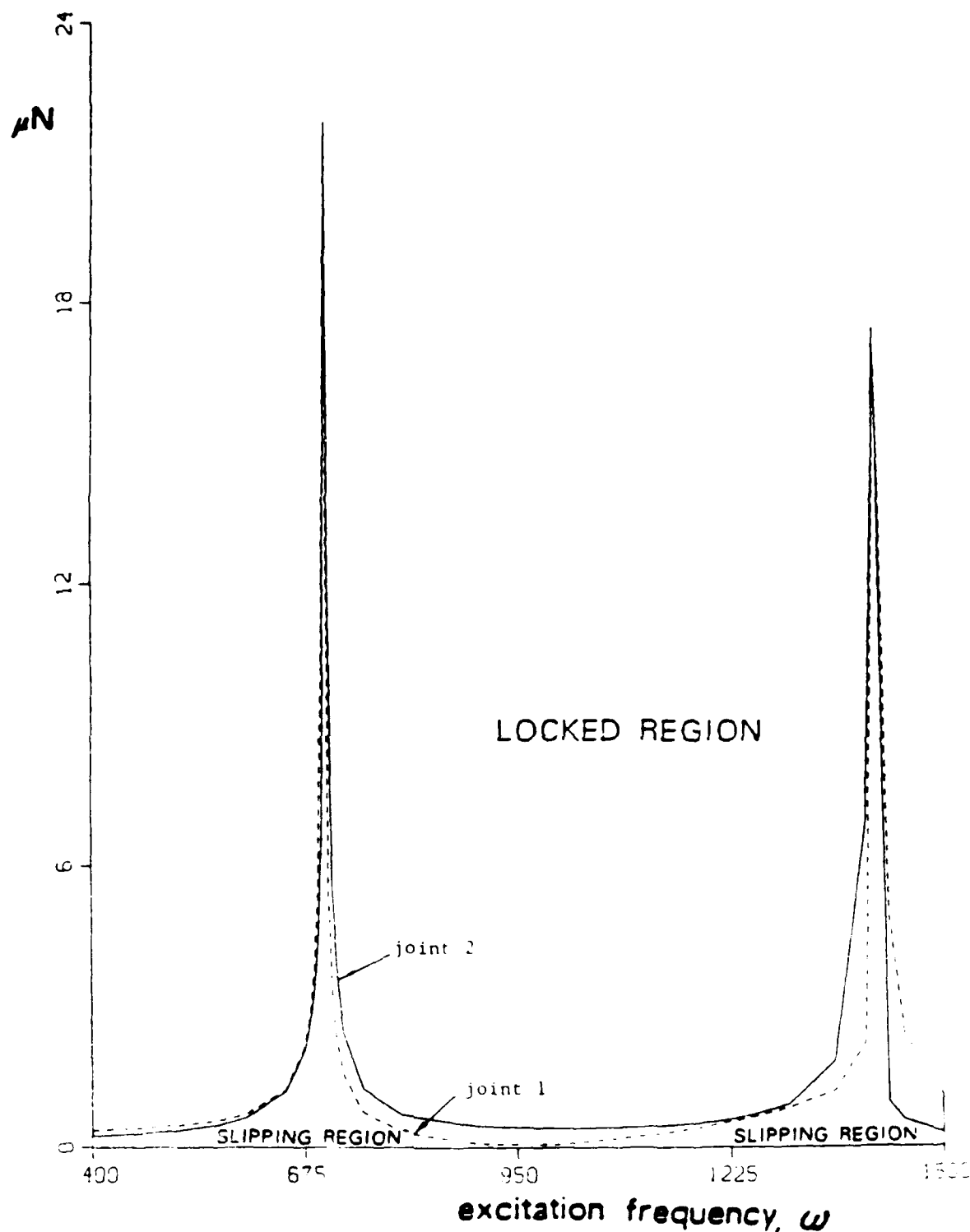
Figure 8: Complete Slip-to-Stuck Curve for System of Fig. 4

28
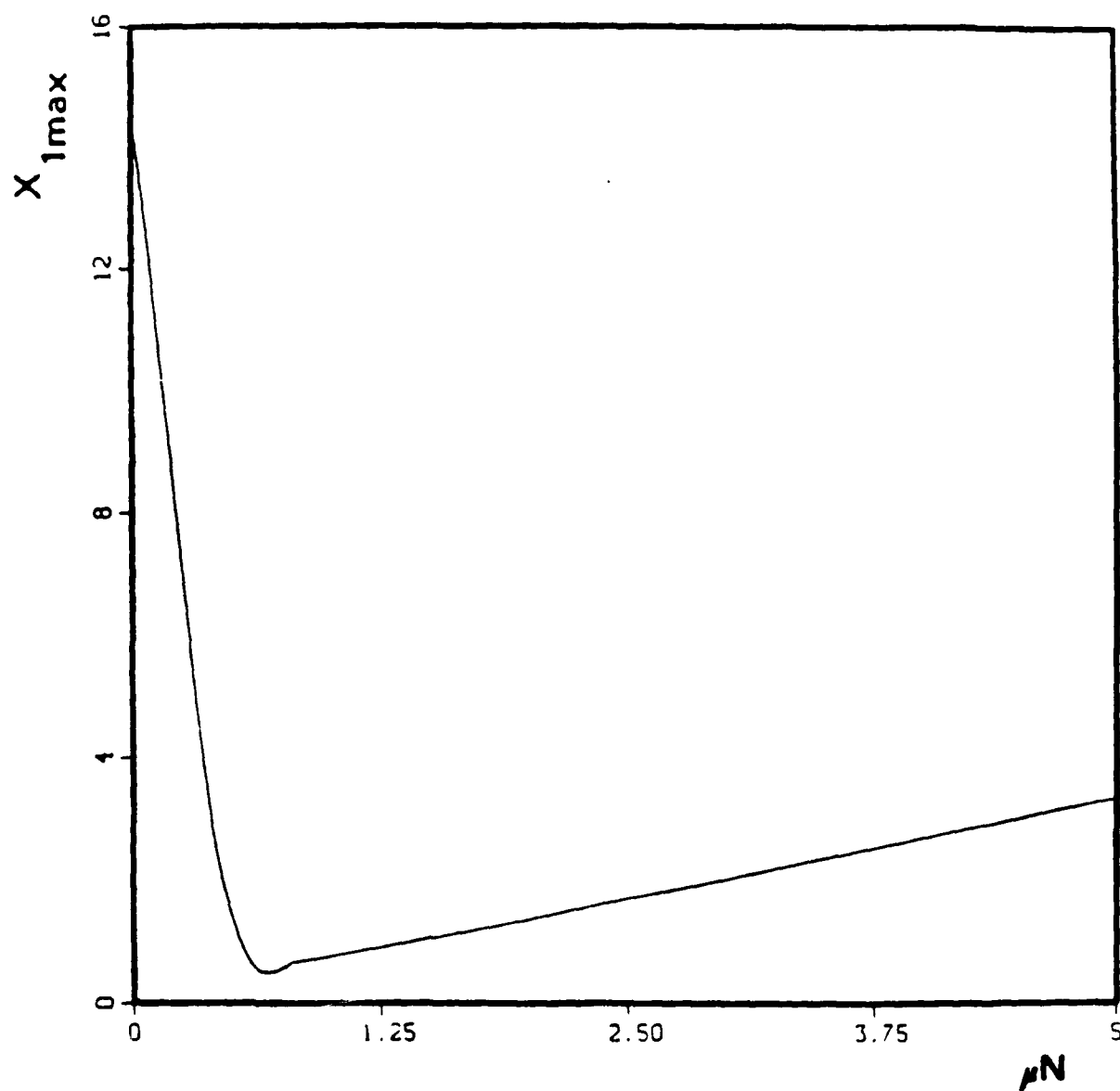
Figure 9:   Optimization Curve for System of Fig. 4

▽ friction joint number

☐ substructure number

○ degree of freedom number
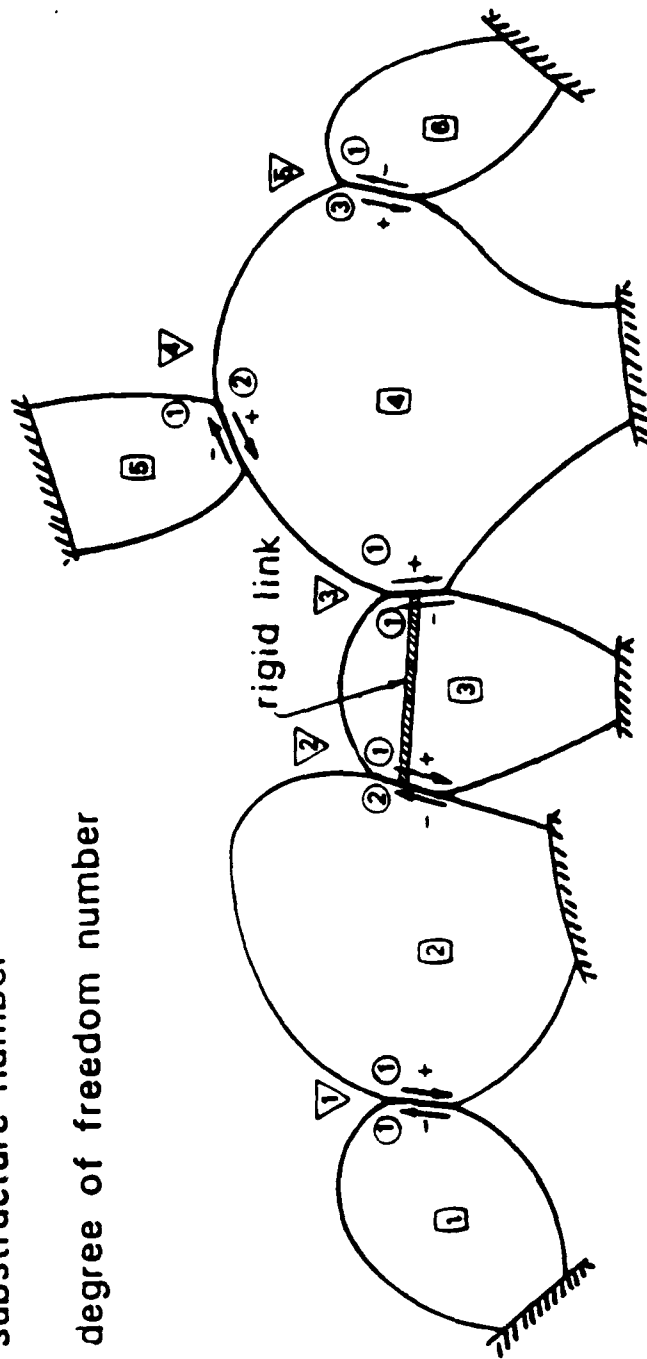
Figure 10: A System of Six Substructures with Five Friction Interfaces
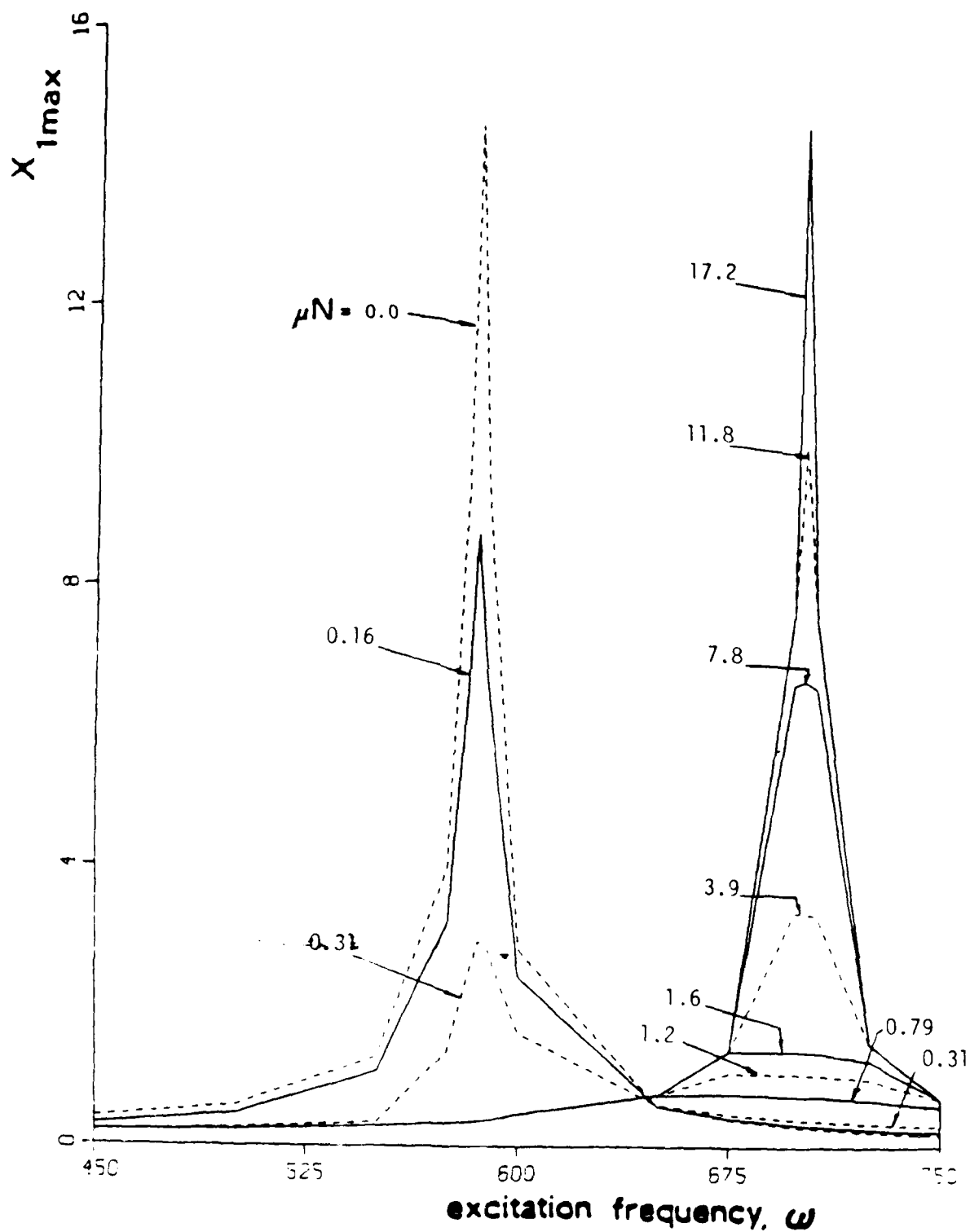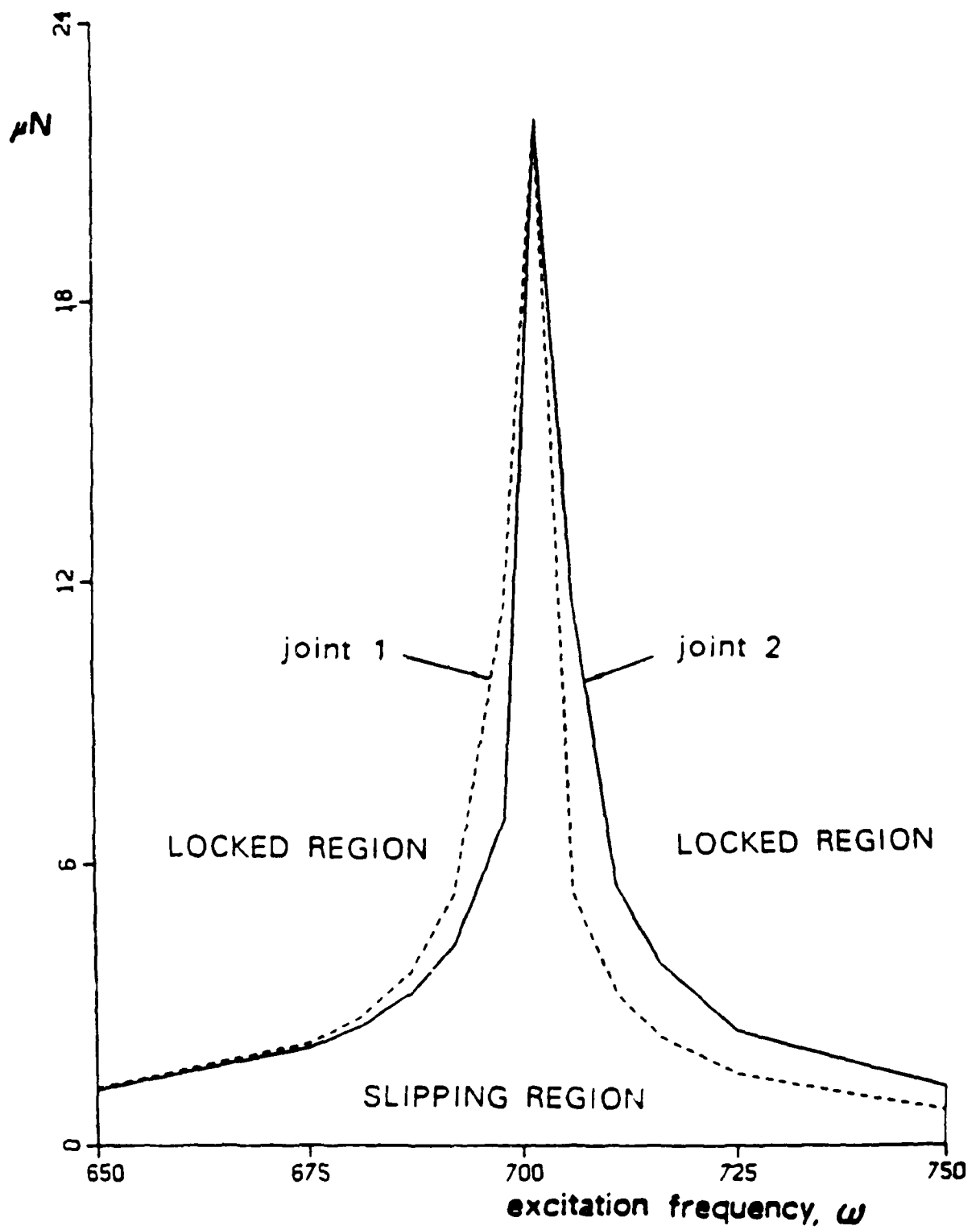
TABLE 1

COMPARISON OF RESULTS FOR THE SYSTEM OF FIG. 3

a) dimensionless frequency ω = 0.707

$\mu N/Q$	relative displacement		displacement of mass 1	
	exact	approx.	exact	approx.
0.20	149.1	149.1	149.0	149.1
0.40	98.0	97.9	98.0	97.9
0.60	46.9	47.2	46.9	47.2
0.80	2.1	-5.6	2.5	2.1
1.00	0.0	0.0	2.0	2.0

b) dimensionless frequency ω = 1.0

$\mu N/Q$	relative displacement		displacement of mass 1	
	exact	approx.	exact	approx.
1.00	3.40	3.61	5.35	6.38
2.40	2.76	3.06	10.93	12.73
6.91	1.36	1.30	30.49	35.24
10.00	0.57	0.12	42.61	50.87
12.50	0.05	0.00	50.93	51.76

∇ friction joint number

◻ substructure number

◯ degree of freedom number
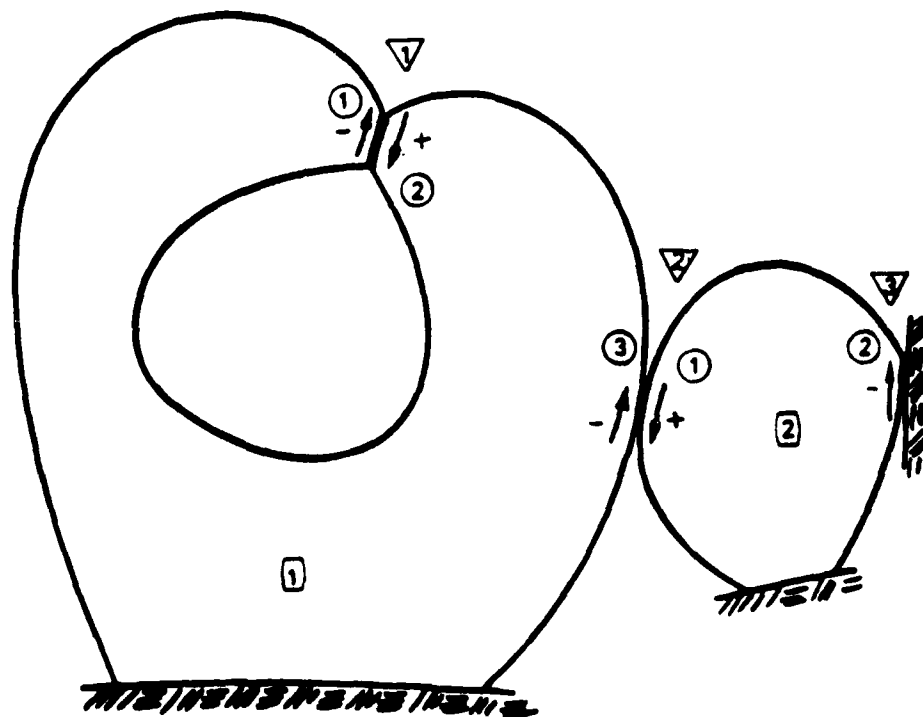
Figure 11: System with a Joint Connected to the Ground and an Internal Interface

31

APPENDIX A. COMPLEX EQUATIONS FOR ILLUSTRATIVE SYSTEMS

A detailed derivation of the complex systems of equations resulting from the application of the methodology is presented in this appendix for the two illustrative systems depicted in Figs. 8 and 9. In order to obtain general rules for deriving the equations for any system, we have tried to include in these examples most of the situations that can occur in practical problems. All the quantities used in this appendix are complex, for clarity, however, the caret $(\hat{\ })$ that denotes complex in the text of the report has been supressed.

1. System of Figure 10

The system of Fig. 10 is a typical case of several structures interconnected by several friction interfaces. The numbers asigned to the substructures, to the friction joints and to the degrees of freedom are indicated in the figure. First, the relative displacements in the joints are defined as follows:

$$d_1 = x_1^2 - x_1^1$$

$$d_2 = x_1^3 - x_2^2$$

$$d_3 = x_1^4 - x_1^3 \qquad\qquad A.1$$

$$d_4 = x_2^4 - x_1^5$$

$$d_5 = x_3^4 - x_1^6$$

These expressions constitute Equations (8) for this system. Equation (7) can be now written for each joint, including the appropiate sign for the friction forces, as follows:

$$x_1^1 = z_1^1 + r_{11}^1 (-f_1)$$

$$\begin{Bmatrix} x_1^2 \\ x_2^2 \end{Bmatrix} = \begin{Bmatrix} z_1^2 \\ z_2^2 \end{Bmatrix} + \begin{bmatrix} r_{11}^2 & r_{12}^2 \\ r_{21}^2 & r_{22}^2 \end{bmatrix} \begin{Bmatrix} +f_1 \\ -f_2 \end{Bmatrix}$$

$$x_1^3 = z_1^3 + r_{11}^3 (+f_2) + r_{11}^3 (-f_3)$$

$$\begin{Bmatrix} x_1^4 \\ x_2^4 \\ x_3^4 \end{Bmatrix} = \begin{Bmatrix} z_1^4 \\ z_2^4 \\ z_3^4 \end{Bmatrix} + \begin{bmatrix} r_{11}^4 & r_{12}^4 & r_{13}^4 \\ r_{21}^4 & r_{22}^4 & r_{23}^4 \\ r_{31}^4 & r_{32}^4 & r_{33}^4 \end{bmatrix} \begin{Bmatrix} +f_3 \\ +f_4 \\ +f_5 \end{Bmatrix}$$

$$x_1^5 = z_1^5 + r_{11}^5(-f_4)$$

$$x_1^6 = z_1^6 + r_{11}^6(-f_5)$$

Define

$$F = \{\, f_1 \quad f_2 \quad f_3 \quad f_4 \quad f_5 \,\}^T \qquad\qquad A.2$$

Now, by using appropiate zero terms, the x_j^s can be expressed in the following form:

$$x_1^1 = z_1^1 + \langle -r_{11}^1 \quad 0 \quad 0 \quad 0 \quad 0 \rangle F$$

$$x_1^2 = z_1^2 + \langle r_{11}^2 \quad -r_{12}^2 \quad 0 \quad 0 \quad 0 \rangle F$$

$$x_2^2 = z_2^2 + \langle r_{21}^2 \quad -r_{22}^2 \quad 0 \quad 0 \quad 0 \rangle F$$

$$x_1^3 = z_1^3 + \langle 0 \quad r_{11}^3 \quad -r_{11}^3 \quad 0 \quad 0 \rangle F$$

$$x_1^4 = z_1^4 + \langle 0 \quad 0 \quad r_{11}^4 \quad r_{12}^4 \quad r_{13}^4 \rangle F \qquad\qquad A.3$$

$$x_2^4 = z_2^4 + \langle 0 \quad 0 \quad r_{21}^4 \quad r_{22}^4 \quad r_{23}^4 \rangle F$$

$$x_3^4 = z_3^4 + \langle 0 \quad 0 \quad r_{31}^4 \quad r_{32}^4 \quad r_{33}^4 \rangle F$$

$$x_1^5 = z_1^5 + \langle 0 \quad 0 \quad 0 \quad -r_{11}^5 \quad 0 \rangle F$$

$$x_1^6 = z_1^6 + \langle 0 \quad 0 \quad 0 \quad 0 \quad -r_{11}^6 \rangle F$$

The quantities between brackets are vectors denoted as r_j^s in expression (7) of the text. In the above form the x_j^s can be replaced into the expressions for the relative displacements A.1 and vector F can be extracted as a common factor. After reordering some terms we obtain equation (9) of the text, i. e.

$$D - RF = Z$$

where

$$D = \{ d_1 \quad d_2 \quad d_3 \quad d_4 \quad d_5 \}^T \qquad\qquad A.4$$

$$R = \begin{bmatrix} (r_{11}^1 + r_{11}^2) & -r_{12}^2 & 0 & 0 & 0 \\ -r_{21}^2 & (r_{22}^2 + r_{11}^3) & -r_{11}^3 & 0 & 0 \\ 0 & -r_{11}^3 & (r_{11}^3 + r_{11}^4) & +r_{12}^4 & +r_{13}^4 \\ 0 & 0 & +r_{21}^4 & (r_{22}^4 + r_{11}^5) & +r_{23}^4 \\ 0 & 0 & +r_{31}^4 & +r_{32}^4 & (r_{33}^4 + r_{11}^6) \end{bmatrix} \qquad A.5$$

$$Z = \left\{ \begin{array}{c} z_1^2 - z_1^1 \\ z_1^3 - z_2^2 \\ z_1^4 - z_1^3 \\ z_2^4 - z_1^5 \\ z_3^4 - z_1^6 \end{array} \right\} \qquad\qquad A.6$$

2. System of Figure 11

This is a system with two substructures and three friction interfaces. The peculiarities distinguishing this system from that of Figure 10 are that two surfaces of one substructure are connected by a internal friction interface, and that the other substructure has a friction interface with the ground. The relative displacements in the joints are

$$d_1 = x_2^1 - x_1^1$$

$$d_2 = x_1^2 - x_3^1$$

$$d_3 = 0 - x_2^2$$

The total displacements of the substructures in nodes connected to friction joints are

$$\left\{ \begin{array}{c} x_1^1 \\ x_2^1 \\ x_3^1 \end{array} \right\} = \left\{ \begin{array}{c} z_1^1 \\ z_2^1 \\ z_3^1 \end{array} \right\} + \begin{bmatrix} r_{11}^1 & r_{12}^1 & r_{13}^1 \\ r_{21}^1 & r_{22}^1 & r_{23}^1 \\ r_{31}^1 & r_{32}^1 & r_{33}^1 \end{bmatrix} \left\{ \begin{array}{c} -f_1 \\ +f_1 \\ -f_2 \end{array} \right\}$$

35

$$\begin{Bmatrix} x_1^2 \\ x_2^2 \end{Bmatrix} = \begin{Bmatrix} z_1^2 \\ z_2^2 \end{Bmatrix} + \begin{bmatrix} r_{11}^2 & r_{12}^2 \\ r_{21}^2 & r_{22}^2 \end{bmatrix} \begin{Bmatrix} +f_2 \\ -f_3 \end{Bmatrix}$$

or

$$x_1^1 = z_1^1 + \langle \; (r_{12}^1 - r_{11}^1) \quad -r_{13}^1 \quad 0 \; \rangle \, F$$

$$x_2^1 = z_2^1 + \langle \; (r_{22}^1 - r_{21}^1) \quad -r_{23}^1 \quad 0 \; \rangle \, F$$

$$x_3^1 = z_3^1 + \langle \; (r_{32}^1 - r_{31}^1) \quad -r_{33}^1 \quad 0 \; \rangle \, F$$

$$x_1^2 = z_1^2 + \langle \quad 0 \quad r_{11}^2 \quad -r_{12}^2 \; \rangle \, F$$

$$x_2^2 = z_2^2 + \langle \quad 0 \quad r_{21}^2 \quad -r_{22}^2 \; \rangle \, F$$

where

$$F = \{ \; f_1 \quad f_2 \quad f_3 \; \}^T$$

Proceeding as in the previous example. i. e. replacing the x_j^i into the expressions for the relative displacements and reordering terms we obtain

$$D - R F = Z$$

This time we have

$$D = \{ \; d_1 \quad d_2 \quad d_3 \; \}^T$$

$$R = \begin{bmatrix} (r_{11}^1 + r_{22}^1 - r_{12}^1 - r_{21}^1) & (r_{13}^1 - r_{23}^1) & 0 \\ (r_{31}^1 - r_{32}^1) & (r_{11}^2 + r_{33}^1) & -r_{12}^2 \\ 0 & -r_{21}^2 & r_{22}^2 \end{bmatrix}$$

$$Z = \begin{Bmatrix} z_2^1 - z_1^1 \\ z_1^2 - z_3^1 \\ -z_2^2 \end{Bmatrix}$$

36

APPENDIX B. DERIVATION OF LINEARIZED EQUATIONS (17) AND (18)

From section 4.2, the vector of increments of friction forces in the joints can be expressed as

$$\Delta \hat{F} = -\imath \left\{ \begin{array}{c} \exp(\imath\theta_1) \ \Delta f_1 \\ \exp(\imath\theta_2) \ \Delta f_2 \\ \vdots \\ \exp(\imath\theta_n) \ \Delta f_n \end{array} \right\} + \imath \left\{ \begin{array}{c} f_1 \Delta\theta_1 \\ f_2 \Delta\theta_2 \\ \vdots \\ f_n \Delta\theta_n \end{array} \right\} \qquad \text{B.1}$$

Define

$$\hat{U} = \begin{bmatrix} \exp(\imath\theta_1) & 0 & \cdots & 0 \\ 0 & \exp(\imath\theta_2) & \cdots & 0 \\ & & & \\ 0 & 0 & \cdots & \exp(\imath\theta_n) \end{bmatrix} \qquad \text{B.2}$$

$$\hat{G} = \begin{bmatrix} f_1 & 0 & \cdots & 0 \\ 0 & f_2 & \cdots & 0 \\ & & & \\ 0 & 0 & \cdots & f_n \end{bmatrix} \qquad \text{B.3}$$

$$\Delta F = \{ \ \Delta f_1 \quad \Delta f_2 \quad \cdots \quad \Delta f_n \ \}^T \qquad \text{B.4}$$

$$\Delta\Theta = \{ \ \Delta\theta_1 \quad \Delta\theta_2 \quad \cdots \quad \Delta\theta_n \ \}^T \qquad \text{B.5}$$

Then B.1 becomes

$$\Delta \hat{F} = -\imath \ \hat{U} \ \Delta F + \imath \ \hat{G} \ \Delta\Theta \qquad \text{B.6}$$

37

Similarly, if we define, in addition,

$$\hat{H} = \begin{bmatrix} \hat{d}_1 & 0 & .... & c \\ 0 & \hat{d}_2 & .... & 0 \\ & & & \\ & & & \\ 0 & 0 & .... & \hat{d}_n \end{bmatrix}$$ B.7

we obtain

$$\Delta D = \{ \ \Delta d_1 \quad \Delta d_2 \quad .... \quad \Delta d_n \ \}^T$$ B.8

the vector of increments of the relative displacements is expressed as

$$\Delta \hat{D} = \hat{U} \ \Delta D \ + \ \imath \ \hat{H} \ \Delta\Theta$$ B.9

Substitution of B.6 and B.9 into Equation (16) yields

$$-\imath \hat{U} \Delta F + \imath \hat{G} \Delta\Theta + \hat{R}(\hat{U}\Delta D + \imath \hat{H}\Delta\Theta) = 0$$ B.10

Note that $\hat{U}$ (defined in A.2) is a unit matrix such that its inverse is also its complex conjugate, i.e., $\hat{U}^{-1} = \hat{U}^*$. Premultiplication of B.10 by $\hat{U}^*$ gives

$$-\imath \hat{U}^* \hat{U} \Delta F + \imath \hat{U}^* \hat{G} \Delta\Theta + \hat{U}^* \hat{R} \hat{U} \Delta D + \imath \hat{U}^* \hat{R} \hat{H} \Delta\Theta = 0$$ B.11

Define now the following real matrices:

$$G = \begin{bmatrix} f_1 & 0 & .... & 0 \\ 0 & f_2 & .... & 0 \\ & & & \\ & & & \\ 0 & 0 & .... & f_n \end{bmatrix}$$ B.12

38

$$H = \begin{bmatrix} d_1 & 0 & \ldots & 0 \\ 0 & d_2 & \ldots & 0 \\ & & & \\ 0 & 0 & \ldots & d_n \end{bmatrix} \qquad \text{B.13}$$

Considering the definitions of $\hat{U}$, $\hat{G}$ and $\hat{H}$ we have

$$\hat{G} = i \, \hat{U} \, G \qquad\qquad \text{B.14}$$

$$\hat{H} = i \, \hat{U} \, H \qquad\qquad \text{B.15}$$

and B.11 can be written as

$$-i\Delta F + iG\Delta\Theta + \hat{U}^*\hat{R}\hat{U}(\Delta D + iH\Delta\Theta) = 0 \qquad \text{B.16}$$

It can be easily verified that the elements of the complex matrix product $\hat{U}^*\hat{R}\,\hat{U}$ are

$$\delta_{nm} = \ell_{nm}\exp[i(\theta_m - \theta_n)] \qquad\qquad \text{B.17}$$

Let B_r and B_i be the real matrices containing the real and the imaginary parts of the terms δ_{nm}, i.e.

$$\hat{U}^*\hat{R}\hat{U} = B_r + iB_i \qquad\qquad \text{B.18}$$

Introducing B.18 into B.16 we have

$$-i\Delta F + G\Delta\Theta + (B_r + iB_i)(\Delta D + i H\Delta\Theta) = 0$$

Equating separately the real and imaginary parts of this equation to zero, equations (17) and (18) of the text are obtained.

APPENDIX C. VERIFICATION OF ALGORITHMS

Algorithms for the automtic derivation of matrix R and vector Z that define the complex system of equations in the methodology proposed in this work are presented in section 6 of the report. The purpose of this Appendix is to illustrate and verify the algorithms by applying them to the representative systems depicted in Figures 10 and 11. Additional rules are also presented for the inclussion of particular cases in the general algorithms, and the required data structures are developed. Even though all the matrices and vectors used in this Appendix are complex the caret (^) used in the text to distinguish these quantities form the real ones have been omited, to obtain a more readable text. The letters denoting the steps are in agreement with those used in the presentation of the algorithms in section 6.

1. System of Fig. 10

a. The numbers assigned to the substructures and to the friction interfaces are presented in Fig. 10. In this case $s = 1,...,6$ and $j = 1,...,5$.

b. The reduced compliance matrices and displacement vectors of the substructures have the following sizes:

substructure, s	size, p
1	1
2	2
3	2
4	3
5	1
6	1

The corresponding matrices, r^s, and vectors z^s are all shown in section 1 of Appendix $A/$, where they were used to write Equations 7 for this system. Substructure 3 is a particular case because the rigid link indicates that the same degree of freedom is connected to two substructures, and consequently the original size of matrix r^3 (1 by 1) does not agree with the size required by the algorithm (2 by 2). To resolve this discreepancy a new, enlarged, matrix r^3 is formed by repeating the original matrix as necessary. Specifically, the original matrix $r^3 = r^3_{11}$, becomes

$$r^3 = \begin{bmatrix} r^3_{11} & r^3_{11} \\ r^3_{11} & r^3_{11} \end{bmatrix}$$

c. The relative displacements in the friction interfaces have been defined at the beginning of section 1 of Appendix A. In tabular form those definitions can be expressed as:

41

joint, j	m	n	i	l
1	2	1	1	1
2	3	2	1	2
3	4	3	1	1
4	4	5	2	1
5	4	6	3	1

d. In agreement with the previous definitions, the incidences vectors, V^s, for the substructures are

$$V^1 = \langle -1 \rangle$$

$$V^2 = \langle +1 \quad -2 \rangle$$

$$V^3 = \langle +2 \quad -3 \rangle$$

$$V^4 = \langle +3 \quad +4 \quad +5 \rangle$$

$$V^5 = \langle -4 \rangle$$

$$V^6 = \langle -5 \rangle$$

V^1 indicates that substructure 1 is connected to friction surface 1 as an "ending" substructure. V^5 and V^6 have a similar interpretation. V^3 shows that the first degree of freedom of substructure 3 is connected to surface 2 as a "starting" value whereas the second degree of freedom is connected to surface 3 as an "ending" value. According to V^4, the three degrees of freedom of the "starting" substructure 4 are connected to surfaces 3, 4 and 5, respectively.

e. Following the rules to form the system compliance matrix, R, for the first substructure we have $u = v = 1$ and $iu = iv = -1$. Therefore, the product $(iu)(iv)$ is positive and r^1_{11} has to be added to R^{11}. Substructure 2 has $u = v = 1,2$ with an incidences vector $\langle 1, -2 \rangle$. We have to add 2x2 terms as indicated in the following table:

u	v	iu	iv	sign of $(iu)(iv)$	add	to
1	1	1	1	+	r^2_{11}	R_{11}
1	2	1	-2	−	r^2_{12}	R_{12}
2	1	-2	1	−	r^2_{21}	R_{21}
2~	2	-2	-2	+	r^2_{22}	R_{22}

A similar table for substructure 3 is:

u	v	iu	iv	sign of (iu)(iv)	add	to
1	1	2	2	+	r^3_{11}	R_{22}
1	2	2	-3	-	r^3_{11}	R_{23}
2	1	-3	2	-	r^3_{11}	R_{32}
2	2	-3	-3	+	r^3_{11}	R_{33}

Performing the additions for the six substructures, the matrix R shown as expression 1.5 in Appendix A is obtained.

f. To form vector Z the term z^1_1 of substructure 1 is added to Z^1 with a minus sign; the term z^2_1 of substructure 2 is also added to to Z^1 but with a positive sign, while the term z^2_2 of the same substructure is added to Z^2 with a negative sign, and so on. The result is expression I.6 of Appendix A.

2. System of Fig. 11

a. The numbers assigned to the substructures and to the friction interfaces are included in Fig. 11. In this case $s = 1,2$ and $j = 1,2,3$.

b. The reduced compliance matrices and displacement vectors of the substructures have the following sizes:

substructure, s	size, p
1	3
2	2

The corresponding matrices, r^s, and vectors z^s are all shown in section 2 of Appendix A.

c. The relative displacements in the friction interfaces have been defined at the beginning of section 2 of Appendix A. In tabular form we have

43

joint, j	m	n	i	l
1	1	1	2	1
2	2	1	1	3
3	0	2	0	2

The "starting" substructure for joint 3 is the ground, which is indicated by assigning zero values to m and i.

d. The incidences vectors, V^s, are

$$V^1 = \langle\ -1 \quad +1 \quad -2\ \rangle$$

$$V^2 = \langle\ +2 \quad -3\ \rangle$$

e. Following the rules to form the system compliance matrix, R, expression I.8 of Appendix A is obtained.

f. The system dispalcements vector Z is expression I.9 of Appendix A.

3. Basic Data Structure

The basic data structure to represent a system with friction interfaces is the table defining the relative displacementes in the joints, namely the table containing m, n, i and l as a function of the joint number, j. The vectors V^s that are used to form R and Z can be constructed automatically from the table using the following rules:

a) The i-th element of vector V^m contains the joint number j with a positive sign;

b) the l-th element of vector V^n contains the joint number j with a negative sign.

c) Apply a) and b) to all the joints. i.e. to all the rows of the table, to obtain all the terms of all vectors V^s.